Journal of Data Acquisition and Processing
ISSN: 1004-9037
https://sjcjycl.cn/
DOI: 10.5281/zenodo.777071

BIO INSPIRED ALGORITHM BASED OPTIMAL DESIGN AND MAXIMUM ENERGY POINT TRACKING IN A GRID CONNECTED SC SYSTEM

Dr.M.Sangeetha [1], Mr.G.Purushothaman [2] , R.Santhi [3], V.Ramesh [4], N.Nivas [5] , K.Vijayaprajesh [6] , M.Viji [7]
Professor [1] , EEE , Assistant professor [2] , PG Student [3] , PG Student [4] , PED , PG Student [5] , PG Student [6] , PG Student [7].
M.A.M. SCHOOL OF ENGINEERING, SIRUGANUR,TRICHY-621105

Abstract
By accurately tracking the maximum energy point (Max-PP), which depends on the board's temperature and the irradiance conditions, maximum energy point tracking (Max-PPT) techniques are utilized as part of SC (SC) designs to increase the SC panel's output energy. To enhance the Max-PPT technique under fractional shading conditions, this paper expands the yield of the SC collection. As part of our suggested approach, a novel technique dubbed the Judgement table (JT) strategy will be utilized to track the SC collection's maximum energy under partial shade conditions, and the extensible particle swarm optimisation (Ex-PSO) algorithm will be utilized to optimise the results. The suggested approach also manages the grid fault. The results show that Ex-PSO based Max-PPT can promote SC collection to achieve the global Max-PP and assist the SC panel in producing more reliable yield management than the standard JT method.
Keywords: Max-PPT; Grid connected SC system, partially shaded conditions; Ex-PSO; J Technique.

1.Introduction

Solar energy systems stand out among other continuously developing renewable energy generation schemes because they provide unrestricted, uncontaminated, and ecologically beneficial energy [1]. This is due to the rapid growth of electrical energy production and energy electronics systems. SC energy stands out as one of the most important energy sources, with increased interest in electrical energy claims that are immaculate, contamination-free, and limitless, while it presently only makes up a very small portion of electrical energy competence and production [2]. One of the most important types of SC context is a grid connected SC (GC-SC) energy system (PS), in which the production of energy depends on a number of variables.

GC-SC frameworks [3] are solar SC PSs that produce electricity and are connected to the utility grid. They are made up of solar panels (SP), one or more inverters, a energy conditioner, and grid connection hardware. Very small amount of energy, primarily single-phase SC "rooftop" systems are utilized for this, and its dedication to the production of clean energy is becoming more widely recognised. One of these frameworks' primary goals [5] is to increase the amount of energy supplied to the grid by controlling the panel's highest Intensity, lowering the switching frequency, and providing high reliability.

GC-SC sources are utilized today [6] in a variety of applications, including household energy supply, battery charging, swimming pool heating systems, water pumping, satellite PSs,

and more. They have the advantage [7] of being sustenance and contamination-free, low adaptation proficiency; because of this, the overall framework expenses will be reduced by using high-competence energy conditioners. Additionally, they are designed to remove the maximum amount of energy possible from the SC phase.

Another technique known as Max-PPT, which depends on the temperature and irradiance states of the panel as well as the load electrical features, has been employed [8] to increase the SC panel yield. For displaying the current-voltage characteristics of the SC panel under linear irradiation, a singular point called Max-PP has been utilized. The Max-PPT controller [9] often runs during the solar unit's dc/dc converter input phase. The innovative DC production from SPs has essentially been translated to the lower voltage needed to regulate the batteries. [10].

The organisation of this article is as follows: Section 2 reviews prior research on the GC-SC model, Section 3 introduces our proposed optimisation methodology, the Ex-PSO algorithm, and comprises the modelling of the projected SC panel using the JT technique, Section 4 illustrates the results and the discussion, and Section 5 concludes the work.

2. Literature Survey

A maximum control Max-PPT technique for GC-SC frameworks without the mediator DC-DC converter phase was published by Antoneta Iuliana Bratcu and Iulian Munteanu [11]. The method made utilize of the erratic signal that typically results from the action of the framework inverter the DC-connect voltage wave.

In [12], Ismail Hossain et al. proposed a clever method for a SC system's Max-PPT under a variety of temperature and insolation conditions, as well as the transformation of the SC energy into a sine wave with a reduced distortion factor (DF) that can be supplied to the grid and utilized to good effect by electrical and microelectronic systems.

Nopporn Patcharaprakiti et al unique .'s approach for Max-PPT using extendable fuzzy logic control for GC-SC schemes was proposed in [13]. A boost converter and a single-phase inverter coupled to a utility grid formed the structure.

Using the neuro-fuzzy network, Aymen Chaouachi et al. [14] described a novel approach for Max-PPT of a GC-SC framework. It was designed to anticipate the recommended SC voltage, ensuring critical energy transfer between the SC creator and the main utility grid. A fuzzy rule-based classifier and three multi-layered feed-forward ANN make up the neuro-fuzzy system.

In Andrés Tobón et al. [15] .'s discussion of Max-PPT optimisation, a SC board is depicted as two diodes. The updated pattern search method was utilized to carry out the enhancement while the customary control was realized using a Sliding Mode Control (SMC).

In the SC age structure arrangement, Y. S. Perdana et al. [16] linked the inclination rate control to the prompt relationship of energy storage devices. To increase the efficiency of the structure and diminish the number of energy converters, the prompt relationship of the super capacitors string and battery amalgamation layout was proposed. The SC structure yield was limited by the energy storage system (ESS) to control the fluctuating rate of SC respect anticipated incline rate regard.

By putting up a robust model farsighted control plan, Adel Merabet et al. [17] examined the incorporation of SC into movement PSs with grid blame ride-through capability. The

control system was installed under normal circumstances and controls the static dc-interface voltage. It also provided the grid with the most spectacular energy trade by regulating the solidarity control factor.

3. Optimal Design of GC-SC system

A. SC model

A semiconductor diode called a SC [15] cell converts solar energy into electrical energy. A SC phase, in actuality, consists of different SC cells. Liable on the application, either a single phase or a series-parallel grouping of different phases might be utilized. The solitary diode SC model, which is the efficient, uncomplicated, and accurate model, serves as the embodiment of the SC phase in this inquiry. Figure 1 shows how this model's identical circuit functions.

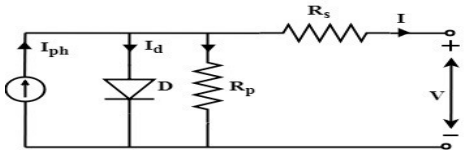

Figure 1. Single diode SC model

The current source, diode, parallel, and series resistances are all included in the single diode SC model. The SC phase's fundamental characteristics have been assembled as follows:

$$I = I_{Ph} - I_{rs}\left[exp\left(\frac{V+R_sI}{f_iV_t}\right) - 1\right] - \frac{V+R_sI}{R_p} \qquad (1)$$

Where $I_{Ph}$is the SC current, $I_{rs}$is the inverse saturation current, $f_i$is the diode critical factor, $R_s$is the sequence resistance, $R_p$is the equivalent resistance, and $V_t = \frac{N_s k\, T}{q}$is the phase thermal voltage.N_s is the quantity of series associated SC cells in the phase, k is the Boltzmann consistent($1.3806503 \times 10^{-23} J/K$), T is the SC phase temperature in Kelvin, and q is the electron charge($1.60217646 \times 10^{-19} C$).$I_{Ph}$is based on the heat contamination[18]. It is communicated by the accompanying condition:

$$I_{Ph} = \left(I_{Ph,n} + SC_I\Delta T\right)\frac{G}{G_n} \qquad (2)$$

Where $I_{Ph,n}$denotes the SC current under the ostensible circumstance (temperature of $25^{\circ}C$ and illumination of 1000 W/m^2), $SC_I$is the SC current per temperature coefficient, ΔT is the contrast between the real and ostensible temperatures, G is the actual heat contamination on the phase surface, and $G_n$is the solar irradiation under the ostensible situation. $I_{Ph,n}$and I_o can be scientifically demonstrated as pursues,

$$I_{Ph,n} = \frac{R_p+R_s}{R_p} I_{sc,n} \qquad (3)$$

$$I_o = \frac{I_{sc,n}+SC_I\Delta T}{exp\left[\frac{(V_{oc,n}+SC_v\Delta T)}{f_iV_t}\right]-1} \qquad (4)$$

Where $I_{sc,n}$, $V_{oc,n}$are the SC and OC voltages under the ostensible condition, respectively. $SC_v$is the open circuit voltage in relation to temperature. The massive SC energy plant is made up of many SC phases that are connected in series and parallel to produce the best yield energy. This SC plant's numerical model can be put together as follows:

$$I = N_pI_{ph} - N_pI_o\left[\exp\left(\frac{V+R_s\left(\frac{N_M}{N_p}\right)I}{N_M\, f_iV_t}\right) - 1\right] - \frac{V+R_s\left(\frac{N_M}{N_p}\right)I}{R_p\left(\frac{N_M}{N_p}\right)} \qquad (5)$$

Where N_M the quantity of series is associated phases in a string and N_p is the quantity of parallel linked strings.

B. Grid Fault Detection

When the voltage dip is identified, the framework should obviously change from usual activity state to grid fault task status. Along these lines, grid control requires a rapid method for identifying voltage sag (VS). In this study, the Root Mean Square (RMS) approach is modified to detect grid faults by registering the RMS estimation of grid voltage (GV) using Eqn. (7) without further modification,

$$U_g = \sqrt{U_{gd}^2 + U_{gq}^2} \qquad (7)$$

Where U_{gd} is the d segment of GV while U_{gq} is the q segment.

C. Reactive Energy (RE) Calculation and Control

The solution to achieve the grid requirement despite the GV dip is to utilize the specified reactive current (RC) computation as the control reference. The ratio of the required RC to the apparent current can be provided piecemeal dependent on the magnitude of VSs.

$$I_{q_{ratio}} = \begin{cases} 0 & , \ U_g > 0.9U_{gn} \\ 2 - 2\frac{U_g}{U_{gn}} & , \ 0.9U_{gn} \geq U_g > 0.5U_{gn} \\ 1 & , \ U_g \leq 0.5U_{gn} \end{cases} \quad (8)$$

Where U_g and U_{gn} are, respectively, the amplitude estimates for the current GV and the standard GV. The location estimate of the RC during the voltage drop (VD) is thus defined as:

$$I_q^* = I_{rated} * I_{q_{ratio}} \quad (9)$$

Where I_{rated} is the estimated current flowing through the grid inverter. The grid inverter's RE reference has been kept at zero during routine operations to attain the unity control factor. Yet, during a grid fault, the grid inverter must broadcast the necessary RE to facilitate GV recovery in accordance with grid requirements. Thus, when the VS is identified, Eqns (8) and (9). will establish the location calculation of the RC.

D. Active Energy (AE) Estimation and Control

When a low-voltage defect arise, there is a brief imbalance between the energy coming from the SC panel and the energy going into the grid, which causes a transient over-current and over-voltage in the SC framework. In this way, reducing the imbalanced energy passing through the SC framework is the main goal of suppressing the over-current and overvoltage. Also, it is essential to generate as much AE as is reasonably possible during VDs to increase the amount of energy captured by the SC panel. The maximum permissible active current allowed to be transmitted to the grid via the grid inverter while faults occur based on the depth of the VS is:

$$I_P = I_{rated} * \sqrt{1 - I_{q_{ratio}}^2} \qquad (10)$$

In the above condition, I_{rated} can be determined by Eq. (8). So the most extreme permitted AE coursing through the grid inverter during faults can be gotten as,

$$P^* = \frac{3}{2} U_g I_P \qquad (11)$$

The boost circuit controller switches from the Max-PPT mode to the non-Max-PPT mode during the GV malfunction. The PI controller has substituted the Max-PPT algorithm in

the non-Max-PPT mode to follow the reference calculation of the AE which is determined by Eqns. 8, 10 and 11. So, the AE inserted into the grid inverter will be managed by the grid inverter's ability to deliver AE during failures, and the extreme energy flowing through the SC framework can be condensed.

E. Proposed Design Strategy

The JT approach is employed in the modelling of Max-PPT systems. The JT block utilizes a range of data to describe important concepts for the yield values. In order to retrieve the equivalent yield values from the table for the known key values, modelling performs a "look-up" task. In the absence of characterising the key values, JT block measures the yield values in light of nearby values.

a) JT technique

Because of the JT technique's [20] usage of the fundamental technique, simplicity, and ease of implementation, it has been chosen to follow the Max-PP of the SC collection. The JT based Max-PPT method produces results relatively quickly and does not necessitate obligatory biasing to obtain the Max-PP because it employs a predetermined table to calculate the Max-PP. Although it can forecast the Max-PP for any number of conditions, the number of sensors required and the number of intended values increase gradually as more conditions are added. This severely restricts how useful utilising such an actual approach.

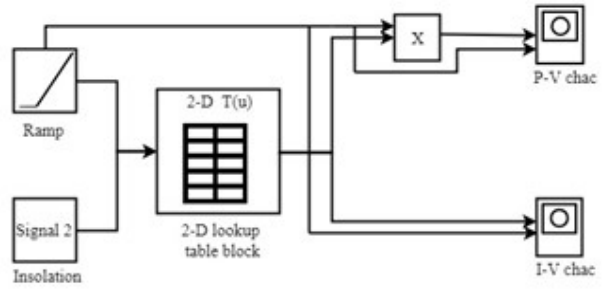

Figure 2: Circuit diagram of Technique

The past data about SC panel, specialised information, and panel qualities at various environmental settings are needed and preserved in the JT procedures. The working point is then switched to a new Max-PP and gathered in the memory of the Max-PPT's framework. At that point, the measured values of the SC panel yield current I-P and output voltage V-P, and the noticed energy is contrasted with the accumulated values to trail the Max-PP. During this task, the corresponding Max-PP for a constraint is selected from memory and run. In this approach, a large amount of data must be kept before finding the Max-PP.

b) JT technique in our proposed methodology

A JT is described for our suggested Max-PPT technique taking the experimental data into account. The I-V and P-V characteristics of the SC phase are monitored using an electronic load, and the results are then obtained using data that has been saved in a digital storage oscilloscope. The P-V curve is utilized to obtain Max-PP at various insulation levels. The judgement table is constructed using data on voltage and current for various insulation levels. The developed model replicates the behaviour of the real SC phase for each given insulation degree. Because the calculations utilized with this model are simple.

c) Ex-PSO Algorithm

PSO is a stochastic, population-based pursuit technique that was established using the behaviour of bird flocks as its model. Every particle in the swarm that the PSO algorithm maintains speaks to a potential solution. Basic behaviour is what particles want to replicate in their interactions with one another and in their own successful endeavours. The best particle in a neighbourhood has an impact on a particle's position p_{best} as well as the best solution found by every one of the particles in the whole populace g_{best}. The particle position P_i is balanced. In PSO, expecting that N particles are introduced arbitrarily, where the i^{th}particle has expressed as (12),

$$P_i = \{P_{i_1}, P_{i_2}, \cdots, P_{i_D}\} \quad (12)$$

The i^{th}particle comes into contact with the current global ideal solution and local ideal solution (optimal position), which can be understood in Eqns (13) and (14) respectively,

$$p_{best} = \{p_{i_1}, p_{i_2}, \cdots, p_{i_D}\} \quad (13)$$

$$g_{best} = \{g_{i_1}, g_{i_2}, \cdots, g_{i_D}\} \quad (14)$$

Flying velocity of the i^{th}particle denoted as (15)

$$V_i = \{V_{i_1}, V_{i_2}, \cdots, V_{i_D}\} \quad (15)$$

Updation of the position and velocity can be spoken to as,

$$V_{ij}^{t+1} = w \cdot V_{ij}^{t} + \varphi_1 r_1 \left(p_{ij}^{t} - P_{ij}^{t}\right) + \varphi_2 r_2 \left(g_{ij}^{t} - P_{ij}^{t}\right) \quad (16)$$

$$P_{ij}^{t+1} = P_{ij}^{t} + V_{ij}^{t+1} \quad (17)$$

Where,w is an inertia weight coefficient utilized to modify the extent of seeking the solution space, t indicates the iterations, φ_1 and φ_2 are the learning variables to adjust the learning step, r_1 and r_2 are the two random numbers which are common as $r_1, r_2 \in [0, 1]$to build the capacity of searching arbitrary. The estimation of $\varphi_1$and φ_2 will be ascertained by utilizing the accompanying conditions,

$$\varphi_1 = \frac{1}{2}(f_{max} + f_{min}) \text{ and} \quad (18)$$

$$\varphi_1 = \frac{1}{2}(f_{max} - f_{min}) \quad (19)$$

Where $f_{max}$is the final fitness value andf_{min} denotes the least fitness value. The inertia weight w can be noted as, in Eqn. (20)

$$w = w_{max} - (w_{max} - w_{min}) \times \frac{t_{current}}{G_{max}} \quad (20)$$

Where, $t_{current}$ is current number of iterations and G_{max} is a predefined maximum number of generations.

The typical PSO algorithm has the benefit of a quick convergence rate, but the disadvantage is that it needs more function evaluations to solve complex multimodal problems and is prone to getting stuck in local optima. The PSO's more extensive applications have been constrained by these flaws. Hence the two most significant and interesting goals in PSO research have evolved into speeding up convergence and avoiding local optima. Ex-PSO is created to strengthen this area of weakness and to accomplish both objectives. The two methods listed below in particular can be employed:

(1) Adjusting parameters depending on knowledge of the particle's current state.

(2) Prediction based on historical data.

The suggested Ex-PSO algorithm is shown in the example below.

Algorithm

Initialize P= $\{P_{i_1}, P_{i_2}, \cdots, P_{i_D}\}$ and $V_i = \{V_{i_1}, V_{i_2}, \cdots, V_{i_D}\}$ $p_{best_{ij}} = P_i$, $t_{current} = 0$, $w = 0.9$.

Calculate φ_1 and φ_2 and g_{best}.

Let $i = 1$.

if$(i \leq N)$

Update P and V

if$(P_{min} \leq P_i \leq P_{max})$

Evaluate particle i and update $p_{best_{ij}}$and g_{best}.

Let $i = i + 1$ and continue step 7.

else let $i = i + 1$ and continue step 7.

else consider $t_{current} = t_{current} + 1$

if$(t_{current} < G_{max})$

go to step 4.

End.

Algorithm 1: Proposed Ex-PSO algorithm

4. IMPLEMENTATION AND RESULTS

MATLAB has been utilized to carry out the suggested strategy. The JT technique was utilized to create the SC collection's I-V and P-V characters, which are depicted in the figures in an incomplete shading situation. The P-V and I-V characteristics separately display the yield energy and current generated by the SC panel.

By using our suggested method, the insulation value is arrived by a reliable block, and the voltage tuning is indicated by a ramp signal, to obtain the I-V and P-V characteristics. Figures 3 and 4 show the I-V and P-V properties acquired using this technique, respectively.

The JT is then provided the estimates for various insulation levels, enabling it to calculate the voltage that corresponds to the given insulation level quickly and easily. To measure the open and short circuit current, a pilot board with similar characteristics to the other boards in the framework can be utilised. The insulation level may be determined from this information, and equivalent information from the judgement table can be obtained. Compared to alternative methods, this method tracks the faster and with less complexity.

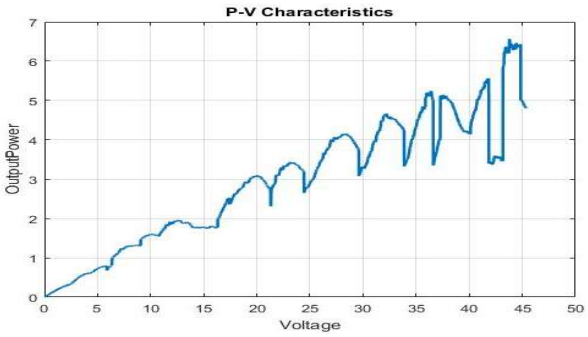

Figure 3: *P-V* characteristic curve of SCpanel

The P-V character from the SC collection is depicted in image 3 above. Based on the voltage of the SC collection, the yield energy is calculated. According to the preceding graph, the output energy increases simultaneously with an increase in the voltage of the SC panel. When the voltage is 45V and we apply our suggested way, the SC panel's maximum energy is 4.9W.

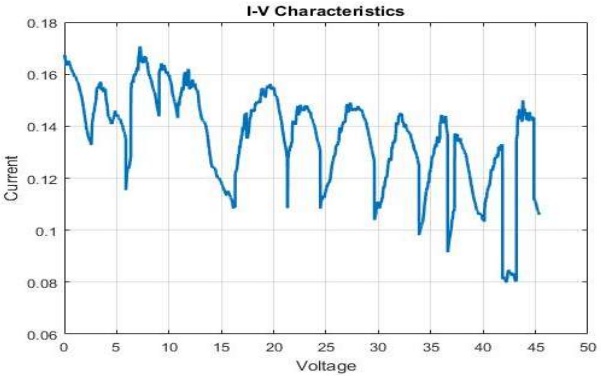

Figure 4: *I-V* characteristic curve of SC panel

Figure 4 utilizes the I-V characteristics curve to illustrate the current that SC collection delivers in a fractionally dark environment. The quantity of voltage will be utilized to determine the current measurement, just like the P-V curve. When the voltage is raised, the equal amount of current will decrease according to the I-V characteristics. Along with the useful operating voltage of 0V to 50V, the amount of current produced is approximately 0.11A.

The normal PSO algorithm is linked to the energy generation of the predicted Ex-PSO method. The JT based Max-PPT responds more quickly, which means that its optimal point locating time is shorter than that of the conventional model, according to the results of the investigation under various test situations. The predicted JT-(Max-PPT) not only reduces the complexity of the entire system but also compresses the tracing time and replication time for multiple interfacing frameworks like GC-SC classifications.

The results of the suggested control test are shown in the following figures for various VS scenarios and times. Figure 5 shows anon-linear single line to ground fault that causes the afflicted phase's voltage at PCC to decrease to 70% in less than 150 milliseconds. Thus, the SC system should supply the grid with 0.6 p.u. of RC and 0.8 p.u. of active current during the fault time (0.45-0.6) s. Hence, adding RE during this period will aid in the voltage recovery. AE, RC, and other values are reset to their pre-fault values after the VS has been eliminated.

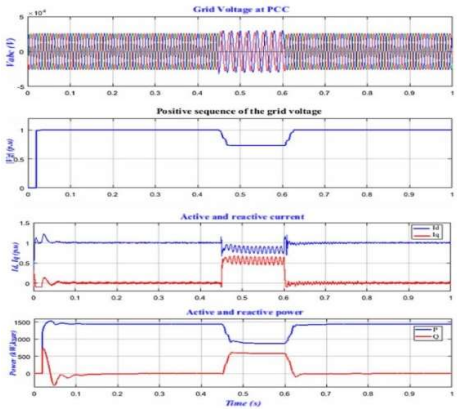

Figure 5: Fault with VD is 30% (VS is 70%) for 625 ms.

A symmetrical three-phase failure is shown in Figure 6 with the greatest possible VD (VS= 15%). In this situation, the standard mandates charging the grid with 100% RC. Hence, the inverter maintains its connection to the grid and supports it with 100% (1 p.u.) RC when the AE is 0.

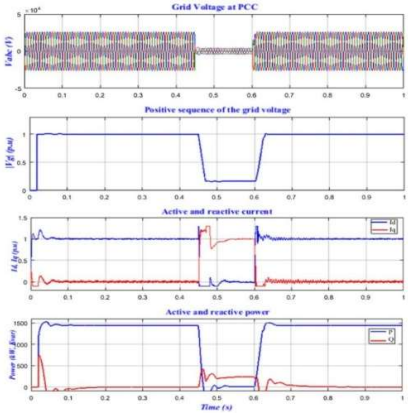

Figure 6**.** Fault with VD is 85% (VS is 15%) for 625 ms.

Figure 7 depicts an unsymmetrical line-to-line (LL) grid failure with a 92% VS and a period of 150 ms. The inverter should remain connected without injecting any RE because the voltage is still in the dead band (between 0.9 p.u and 1.1 p.u), and the voltage at the affected phases is more than 90% of the nominal voltage (V pg>0.9 V gn). The generation of AE should also continue at full capacity based on the weather. Although a VS has been identified, the inverter is still connected for the length of the fault ride-through despite not supplying any RE.

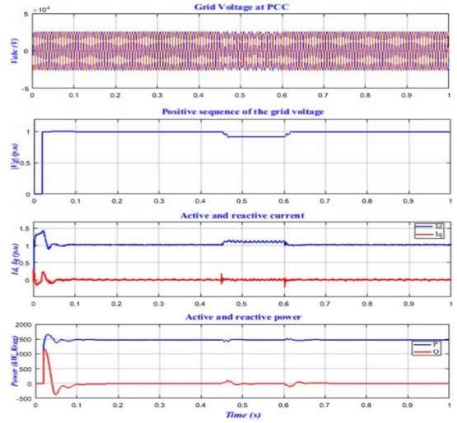

Figure 7: Fault with VD is 8% (VS is 92%) for 625 ms.

Figure 8 shows how the inverter grid control system responded to a two-line to ground (2LG) fault that caused the voltage to drop to 60% of its nominal value. According to grid requirements, the inverter should support 100% (1p.u) responsive current with a 40% drop in voltage. It is clear from the numbers that the inverter maintained the grid with the necessary respect. As the grid is receiving 100% of the receptive current, there is no dynamic current and hence no dynamic energy. The VDs to 30% of its stated value when a fair three-stage voltage decrease (70%) occurs at the grid side for 625 milliseconds.

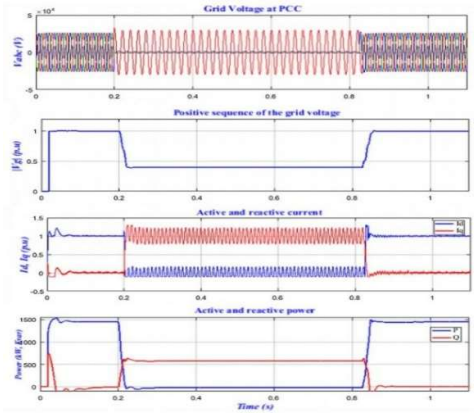

Figure 8. Fault with VD is 60% (VS is 40%) for 150 ms.

5. CONCLUSION

To quickly locate Max-PP under a variety of lighting conditions, this paper investigates the SC array performance utilising Ex-PSO based JT approach. Once the SC array is present in partially shadowed situations, the energy generation of the suggested PSO-based JT is studied. Moreover, it lessens the SC interfacing scheme's computing requirements. With the JT approach, electrical load is utilized to coerce the necessary data from the realistic characteristic. The JT is created in MATLAB and put to the test with varying illumination restrictions. The suggested Ex-PSO based JT's output energy generation is equal to that of the traditional PSO in terms of output energy. The proposed method attempted to maintain voltage at defined values under normal conditions and reduced voltage fall in the error situation. Thus, the SC energy plants can contribute to the stability and dependability of the grid.

REFERENCES

[1] R. Bakhshi and J. Sadeh, ‘‘A comprehensive economic analysis method for selecting the SCpanel structure in grid–connected SC systems,’’ Renew. Energy, vol. 94, pp. 524–536, Aug. 2016.

[2] M.-H. Tan, T.-K. Wang, C.-W. Wong, B.-H. Lim, T.-K. Yew, W.-C. Tan, A.-C. Lai, and K.-K. Chong, ‘‘Optimization study of parasitic energy losses in SC system with dual-axis solar tracker located at different latitudes,’’ Energy Procedia, vol. 158, pp. 302–308, Feb. 2019.

[3] C. O. Okoye, A. Bahrami, and U. Atikol, ‘‘Evaluating the solar resource potential on different tracking surfaces in nigeria,’’ Renew. Sustain. Energy Rev., vol. 81, pp. 1569–1581, Jan. 2018.

[4] K. Mansaray, ‘‘TTechno-economic assessment of a biomass-based hybrid energy system for rural electrification in Sierra Leone,’’ Res. Gate, vol. 9001, pp. 1–8, Aug. 2016.

[5] Öztürk, S., & Çadırcı, I. (2018). A generalized and flexible control scheme for SC grid-tie micro-inverters. IEEE Transactions on Industry Applications, 54(1), 505-516.

[6] Hasanien, Hany M. "Performance improvement of SCPSs using an optimal control strategy based on whale optimization algorithm." Electric PSs Research 157 (2018): 168-176.

[7] Qiu, Y., Yuan, C., & Tang, J. (2018). Integrating SCESS into a Ship-SCPS to Mitigate Energy Fluctuations and Improve GRID Capability. Arabian Journal for Science and Engineering, 1-13.

[8] Perdana, Yoga, et al. "Direct Connection of Supercapacitor-Battery Hybrid Storage System to the Grid-tied SC System." IEEE Transactions on Sustainable Energy (2018).

[9] Merabet, Adel, Labib Labib, and Amer MYM Ghias. "Robust model predictive control for SC inverter system with grid fault ride-through capability." IEEE Transactions on Smart Grid 9.6 (2018): 5699-5709..

[10] Tafti, Hossein Dehghani, et al. "Flexible Control of SC Grid-Connected Cascaded H-Bridge Converters During Unbalanced VSs." IEEE Transactions on Industrial Electronics 65.8 (2018): 6229-6238.

[11] Moghadasi, Amir, et al. "A Model Predictive Energy Control Approach for a Three-Phase Single-Stage Grid-Tied SCPhase-Integrated Converter." IEEE Transactions on Industry Applications 54.2 (2018): 1823-1831.

[12] Errouissi, Rachid, and Ahmed Al-Durra. "Disturbance Observer-Based Control for Dual-Stage Grid-Tied SC System under Unbalanced GVs." IEEE Transactions on Industrial Electronics (2018).

[13] Munteanu, Iulian, and AntonetaIulianaBratcu. "MPPT for GC-SCsystems using ripple-based Extremum Seeking Control: Analysis and control design issues." Solar Energ*y*, vol.111, pp.30-42, 2015.

[14] Hossain, Md Ismail, ShakilAhamed Khan, Md Shafiullah, and Mohammad Jakir Hossain. "Design and implementation of MPPT controlled grid connected SC system." In IEEE Symposium on Computers & Informatics (ISCI), 2011, pp. 284-289. IEEE, 2011.

[15] Tobón, Andrés, Julián Peláez-Restrepo, Juan Villegas-Ceballos, Sergio I. Serna-Garcés, Jorge Herrera, and AsierIbeas. "Maximum Energy Point Tracking of SC Panels by Using Improved Pattern Search Methods." Energies, vol.10, no.9, pp.1316, 2017.

[16] [Sampaio, Priscila GonçalvesVasconcelos, and Mario Orestes Aguirre González. "SC solar energy: Conceptual framework." Renewable and Sustainable Energy Reviews, vol.74, pp.590-601, 2017.

[17] Abdelsalam, Ahmed K., Ahmed M. Massoud, Shehab Ahmed, and Prasad N. Enjeti. "High-performance extensible Perturb and Observe MPPT technique for SC-based microgrids." IEEE Transactions on Energy Electronics, vol.26, no.4, pp.1010-1021, 2011.

[18] Putri, Ratna Ika, Sapto Wibowo, and Muhamad Rifa’i. "Maximum energy point tracking for SC using incremental conductance method." Energy Procedia, vol.68, pp.22-30, 2015.

[19] Ishaque, Kashif, Zainal Salam, Muhammad Amjad, and Saad Mekhilef. "An improved particle swarm optimization (PSO)–based MPPT for SC with reduced steady-state oscillation." IEEE transactions on Energy Electronics, vol.27, no.8, pp.3627-3638, 2012.

[20] Teshome, D. F., C. H. Lee, Y. W. Lin, and K. L. Lian. "A modified firefly algorithm for SC maximum energy point tracking control under partial shading." IEEE Journal of Emerging and Selected Topics in Energy Electronics, vol.5, no.2, pp.661-671, 2017.

[21] Tazi, S. N., Mukesh Gupta, and Akansha Jain. "A survey on application of nature inspired algorithms." *International Journal of Computer Science Engineering* 4.4 (2014): 33-40.

[22] JALADI, SATYENDRA, and T. E. Rao. "An inverse kinematics analysis of space station remote manipulator system (SSRMS) using genetic algorithms." *International Journal of Mechanical and Production Engineering Research and Development* 9.1 (2019): 217-226.

[23] Danthala, S. W. E. T. H. A., et al. "Robotic manipulator control by using machine learning algorithms: A review." *International Journal of Mechanical and Production Engineering Research and Development* 8.5 (2018): 305-310.

[24] MINH, DANG HOANG, P. H. U. N. G. VAN BINH, and NGUYEN VIET DUC. "Multi-objective design for a new type of frame saw machine." *International Journal of Mechanical and Production Engineering Research and Development* 9.2 (2018): 449-466.

[25] Deshpande, Soham G., and N. Bhasme. "Modeling and Simulation of Microinverter with Flyback Converter for grid connected PV systems." *International Journal of Electrical and Electronics Engineering Research* 7.4 (2017): 71-82.

[26] Rao, KV Govardhan, and P. Babu Rao. "A Novel Hybrid PV/FC Energy Management Scheme For Grid Connection And Islanded Operation Capabilities." *International Journal Of Electrical & Electronics Engineering Research (IJEEER)* 4.05 (2014): 13-26.